

Kinetics and Thermodynamics of Heavy Metal Cu(II) Adsorption on Mesoporous Silicates

Ping Ge^{1,2}, Fengting Li^{1*}

¹State Key Lab of Pollution Control and Resource Reuse Study

²College of Environmental Science and Engineering

Tongji University, 200092 Shanghai, China

Received: 19 March 2010

Accepted: 1 July 2010

Abstract

Investigations were conducted to study the adsorption behavior of heavy metal Cu(II) on the mesoporous silicate SBA-15 (CONH₂-SBA-15) in aqueous medium by varying parameters such as contact time, temperature, ionic strength, and competing ions. Heavy metal adsorption was broadly independent of initial metal concentration. Competing ions in the aqueous solution had a small effect on the adsorption of Cu(II) on CONH₂-SBA-15. The adsorption data for Cu(II) fit well with the Langmuir and Redlich-Peterson models. Kinetic studies showed that the kinetic data are well described by the pseudo second-order kinetic model. Initial adsorption rate increases with an increase in temperature. The intraparticle diffusion model was the best in describing the adsorption kinetics for the Cu(II) on CONH₂-SBA-15. Thermodynamic analysis indicates that the adsorption is spontaneous and endothermic.

Keywords: Cu(II), mesoporous materials, adsorption isotherm, adsorption kinetics, adsorption thermodynamics

Introduction

Heavy metal ions have attracted much attention due to their toxicity [1-3]. Contamination by heavy metals occurs in the aqueous waste streams of several industries, such as metal finishing, mining and mineral processing, coal mining, and oil refining and tanneries, among others [4]. Some metals associated with these activities are: cadmium, copper, chromium, iron, mercury, nickel, lead, and zinc [5]. It is important to note that copper is one of the toxic metals that slowly accumulate in the bodies of living creatures. In China, the maximum recommended level of Cu²⁺ in surface water is 0.1 mg/L.

Selective adsorption has become increasingly important in recognition, sensing, and separation of molecules and ions. Adsorption is the process by which a solid adsorbent

can attract a component in water to its surface and form an attachment *via* a physical or chemical bond, thus removing the component from the fluid phase. Some advantages of the adsorption process are simplicity in operation, low cost compared to other separation methods and no sludge formation [6].

Mesoporous materials have been synthesized for various applications such as adsorption, catalysis, and semiconductors [7-9]. In particular, functionalization of mesoporous materials can provide chemical affinity for specific guest molecules and improved dispersion in aqueous solution [10-13].

In this paper, the adsorption kinetics and thermodynamics were studied under various conditions and the adsorption equilibria were investigated to find out which isotherm model best fits the experimental data. The effects of the adsorbate temperature, pH and other ions were studied in order to determine the optimal adsorption conditions.

*e-mail: fengting@mail.tongji.edu.cn

Experimental

The Mesoporous Silicates

The synthesis of adsorbent A was carried out in accordance with the published paper [14], with triblock copolymer (Pluronic P123, $\text{EO}_{20}\text{PO}_{70}\text{EO}_{20}$, $M_{av}=5800$) and cetyltrimethylammonium bromide (CTAB) as hybrid surfactant templates, and tetraethyl orthosilicate (TEOS, 98%, $M_{AV}=208.33$) as the silica source. The typical synthesis process was as follows: 4 g P123 and 0.5 g CTAB were dissolved in 40 g dry ethanol and 0.4 g HCl at room temperature and stirred for 2 h. At the same time, 2.22 g A-1160, and 20 g dry ethanol were mixed and also stirred for 2 h. Then 6.6 g TEOS was slowly added into the mixed solution of the above two to obtain a gel (The molar composition of the mixture was 0.022 P123:0.015 CTAB:1 Teos:6.25 H_2O :0.025 HCl:40.76 ethanol). After 1 h of stirring, the resulting gel was transferred into a Petri dish for solvent evaporation. The slurry produced was transferred into a polypropylene bottle at 90°C for 3 d under static conditions. After filtration, it was then submitted to a continuous reflux run overnight in ethanol/HCl at 70°C to extract the surfactant templates. Then it was filtered, neutralized by stirring with 1 mol/L NaHCO_3 solution for 24 h, and washed with deionized water. Finally, it was dried under vacuum.

The Heavy Metals

In the adsorption experiments, metal nitrates (analytical grade) were dissolved in pure water in order to prepare initial metal ion solutions with different concentrations (0.5, 0.8, 1, 2, 3, 4, 5, 6 mmol/L, respectively).

The Adsorption Studies

In a typical run, approximately 50 mg of mesoporous silica and 10 ml of metal ion solution were placed in a stoppered vial and subjected to ultrasonic irradiation for 25 min at room temperature. Solution pH was adjusted with dilute HCl and NaOH solutions, and the solution ionic strength was adjusted with KNO_3 solution. Metal concentration change was recorded by ICP/OES spectroscopy.

The amount of metal adsorbed onto the mesoporous silicas was calculated by a simple mass balance relationship:

$$Q = (C_0 - C_e) \times \frac{V}{W} \quad (1)$$

Results and Discussion

Effect of Ionic Strength

The effect of ions on the equilibrium adsorption amount is shown in Fig. 1. It shows that the adsorption was affected by the ions in solution. The adsorption order of Cu^{2+} in the presence of the other ions is $\text{NO}_3^- > \text{H}_2\text{O}$ (pure water

–blank) $> \text{NH}_4^+ > \text{SO}_4^{2-} > \text{Cl}^-$ and only the Cl^- affected the adsorption significantly.

Effect of Competitive Adsorption

The divalent cations Cd^{2+} , Ni^{2+} , and Co^{2+} were selected as competing ions with Cu^{2+} because those cations are divalent and have similar ionic radii.

A selectivity coefficient ($P_{a/b}$) for the binding of Cu^{2+} in the presence of other metal ions was calculated according to Eq. (2)

$$P_{a/b} = \frac{P_a}{P_b} \quad (2)$$

...where $P_{a/b}$ represents the ratio of the value of P_a of Cu^{2+} to P_b (Cd^{2+} , Ni^{2+} , Co^{2+}) in mixed solutions.

Table 1 summarizes the values for the distribution constants (P_a) and selectivity coefficients $P_{a/b}$ of $\text{CONH}_2\text{-SBA-15}$ toward Cu^{2+} in the presence of other metal ions. It was observed that almost all the $P_{a/b}$ values were greater than 2.

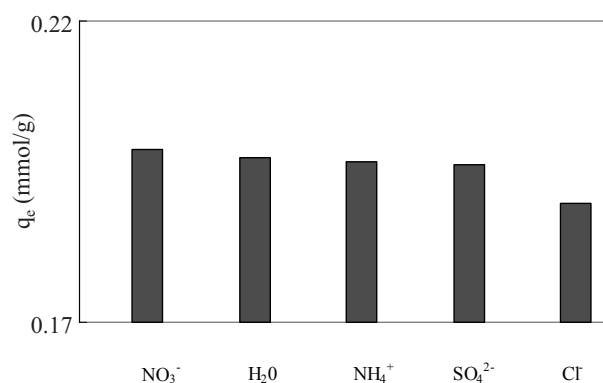


Fig. 1. Effect of ionic strength on the adsorption.

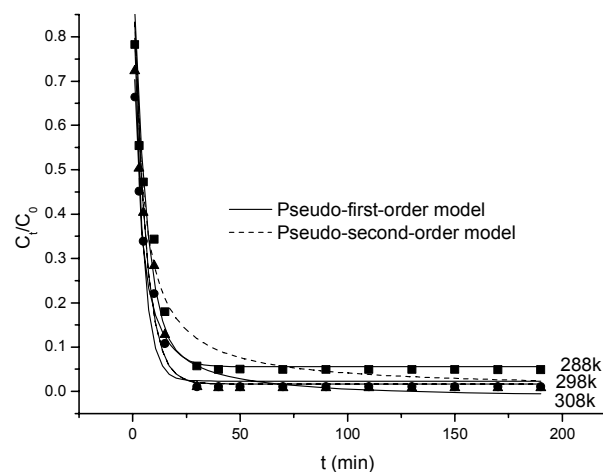


Fig. 2. The relationship between C_t/C_0 and t for the first-order adsorption model and second-order adsorption model at different temperatures (288K, 298K, 308K) of $\text{Cu}(\text{II})$

Table 1. Cu(II) adsorption on CONH₂-SBA-15 in the presence of other metal ions (25°C, pH 5.0).

Heavy metals		C_a	C_b	Q_a	Q_b	$P_{a/b}$
a+b		(mmol/L)	(mmol/L)	(mmol/g)	(mmol/g)	
Cu	Pb	0.01800	0.02100	0.1960	0.1995	1.221
Cu	Zn	0.02700	0.05900	0.1950	0.1880	2.310
Cu	Ni	0.01500	0.04500	0.1970	0.1910	3.094
Cu	Co	0.03610	0.6482	0.1920	0.0703	49.10
Cu	Cd	0.01420	0.4790	0.1970	0.1040	63.76

This suggests that the competing ions in the aqueous solution had a small effect on the adsorption of Cu(II) on CONH₂-SBA-15.

Adsorption Isotherm

The adsorption isotherm experimental data collected at different heavy metal concentrations and various temperatures were fitted with three adsorption models: Langmuir, Freundlich, and Redlich-Peterson isotherm models [15-18].

The Langmuir equation is given as:

$$q_e = \frac{QKC_e}{1 + KC_e} \tag{3}$$

...where q_e is the sorption capacity of adsorbents at equilibrium (mmol/g); Q is the constant, sorption capacity of adsorbents (mmol/g); K is the Langmuir constant (L/mmol); C_e is the concentration of adsorbate at equilibrium (mmol/L).

The Freundlich equation is given as:

$$q_e = K_F C_e^{\frac{1}{n}} \tag{4}$$

...where K is the Freundlich constant; n is a constant, often >1.

The Redlich-Peterson equation is given as:

$$q_e = \frac{K_R C_e}{1 + \alpha C_e^\beta} \tag{5}$$

...where K , α are the Redlich-Peterson constants; β is the index.

The graphically calculated Q , K , and R^2 (Langmuir isotherm), n , K_F , and R^2 (Freundlich isotherm), K_R , α , β , and R^2 (Redlich-Peterson) are regrouped in Table 2. Comparison of the three adsorption models shows the Redlich-Peterson isotherm to be the best model for the metals. Theoretically calculated Q values that are the maximum monolayer capacities of the adsorbent are 1.491, 1.404, and 1.299 mg/g for the experiments performed at 288K, 298K, and 308K, respectively.

Adsorption Kinetic Models

Both pseudo first- and second-order adsorption models were used to describe the sorption kinetics data [19, 20]. In both models, all the steps of adsorption such as external diffusion, internal diffusion, and adsorption are lumped together and it is assumed that the difference between the average solid phase concentration and the equilibrium concentration is the driving force for adsorption, and that the overall adsorption rate is proportional to either the driving force (as in the pseudo first-order equation) or the square of the driving force (as in the pseudo second-order equation).

First-order model:

$$\frac{C_t}{C_0} = \left(1 - \frac{m_s q_e}{C_0}\right) + \frac{m_s q_e}{C_0} e^{-k_1 t} \tag{6}$$

Second-order model:

$$\frac{C_t}{C_0} = 1 - \frac{m_s q_e}{C_0} \cdot \frac{q_e k_2 t}{1 + q_e k_2 t} \tag{7}$$

In these two equations, C_0 and C_t are the initial and liquid-phase concentrations of adsorbates (mmol/L), respec-

Table 2. Langmuir, Freundlich, Redlich-Peterson coefficients for adsorption of Cu(II) onto mesoporous materials.

T(K)	Langmuir			Freundlich			Redlich-Peterson			
	R^2	Q	K	R^2	K_F	$1/n$	R^2	K_R	α	β
288	0.9920	1.491	19.73	0.9920	3.009	0.5007	0.9984	54.70	23.68	0.7060
298	0.9826	1.404	26.45	0.9956	2.830	0.4545	0.9971	171.3	67.47	0.6202
308	0.9734	1.299	44.95	0.9960	2.826	0.4147	0.9984	309.7	124.2	0.6523

Table 3. Comparison of experiments and kinetic models.

T(K)	first-order adsorption model			Second-order adsorption model		
	R^2	q_e	k_1	R^2	q_e	k_2
288	0.9682	0.1889	0.2345	0.9818	0.1992	1.288
298	0.9535	0.1967	0.2764	0.9822	0.2014	1.624
308	0.9387	0.1953	0.2935	0.9856	0.2037	2.016

tively, at any time t , q_e is the equilibrium adsorption (mmol/g) (q_e has previously been used for dye adsorption value), m_s is the adsorbent concentration (g/L).

The plots C_t/C_0 and t were used to test the first- and second order models, and the fitting results are given in Table 3. According to the correlation coefficients, both models give satisfactory fits. But the calculated adsorption amount at equilibrium shows a difference. Comparison of the two kinetic models shows the second-order adsorption model to be a better fitting model for metals adsorption.

Internal Diffusion Analysis

The adsorption process on a porous adsorbent generally involves three stages:

- (i) external diffusion;
- (ii) internal diffusion (or intra-particle diffusion);
- (iii) actual adsorption [21, 22].

Quantitative treatment of experimental data may reveal the predominant role of a particular step among the three that actually governs the adsorption rate. The adsorption step is usually very fast for the adsorption of heavy metals on mesoporous adsorbents compared to the external or internal diffusion step [23], and it is known that the adsorption equilibrium is reached within several minutes in the absence of internal diffusion [24]. Thus, the long adsorption equilibrium time in our experiments (1-3 hours) suggests that internal diffusion may dominate overall adsorption kinetics.

Because the above pseudo models do not provide definite information on the rate-limiting step, an internal diffusion model based on Fick's second law is used to test if the internal diffusion step is the rate-limiting step [25]:

$$q_t = k_p t^{1/2} + C \quad (8)$$

According to the internal diffusion model, a plot of q_t versus $t^{1/2}$ should give a straight line with a slope k_p and an intercept of zero if the adsorption is limited by the internal diffusion process [26]. The relationship between q_t and $t^{1/2}$ at different temperatures is shown in Fig. 3. Initially in all the cases studied, a linear relationship between q_t and $t^{1/2}$ with a zero intercept is found, suggesting that the internal diffusion step dominates the adsorption process before equilibrium is reached.

Fig. 3 shows the plot of q_t versus $t^{1/2}$, which clearly shows all the data follow the same kinetics. This confirms

that the adsorption process can be described by a simple internal diffusion model; internal diffusion was found to be the rate-limiting step.

Thermodynamic Parameter Estimation

The Gibbs free energy change of the adsorption process is related to the equilibrium constant by the following equation:

$$\ln k = -\frac{E_a}{RT} + B \quad (9)$$

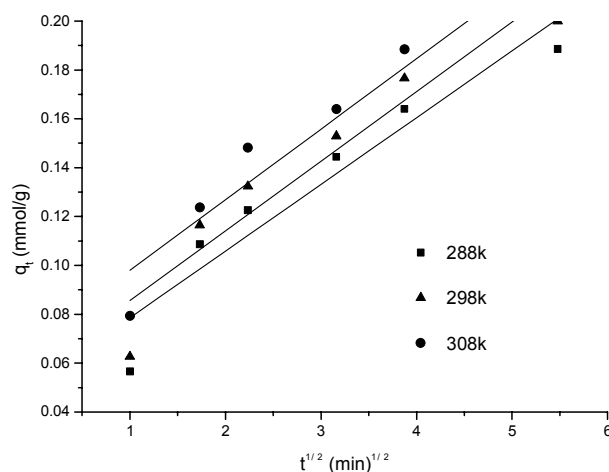


Fig. 3. Plot of q_t vs. $t^{1/2}$ in internal diffusion model.

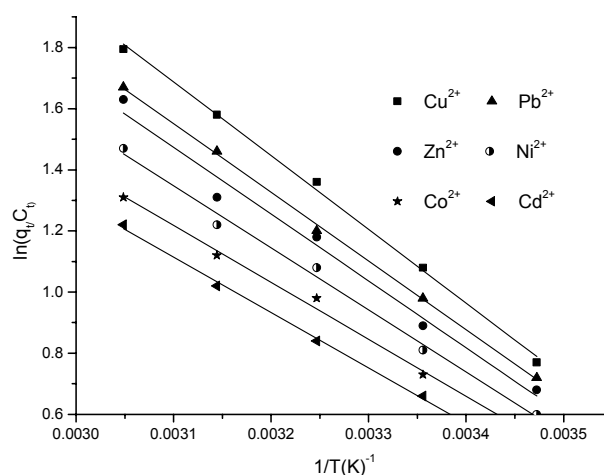


Fig. 4. Plot of $\ln(q_t/C_t)$ vs. $1/T$.

Table 4. Thermodynamic parameters for the adsorption.

metals	ΔH	ΔS	R^2	ΔG		
				288 K	298 K	308 K
Cu	20.07	76.26	0.9978	-1.890	-2.652	-3.415

The enthalpy change (ΔH) and entropy change (ΔS) for adsorption are assumed to be temperature independent and the Gibbs free energy change (ΔG) is related to the enthalpy and entropy change by the following equations:

$$\Delta G = \Delta H - T\Delta S \quad (10)$$

$$\ln \frac{q_t}{C_t} = \frac{\Delta S}{R} - \frac{\Delta H}{RT} \quad (11)$$

A study of the temperature dependence of adsorption gives valuable information about the enthalpy and entropy changes during adsorption. The relationship between q_t/C_t and $1/T$ is given in Fig. 4. The estimated adsorption thermodynamic parameters are listed in Table 4.

The negative value of ΔG indicates that the adsorption of metal Cu(II) on the xerogel is spontaneous for the temperature range evaluated, which is usually the case for many adsorption systems in solution. The positive value of ΔH shows that the adsorption is endothermic, so raising the temperature leads to a higher adsorption of Cu(II) at equilibrium. The positive value of ΔS indicates a process impacted by "promoting the entropy"

Conclusions

The use of a mesoporous hybrid xerogel for the adsorption of an organic dye from aqueous solution has been examined. The results are summarized as follows:

- (1) The adsorption kinetics can be well described by the pseudo second-order kinetic model. Initial Equilibrium time decreases with increases in temperature.
- (2) The internal diffusion of Cu(II) into the mesoporous materials is the rate-limiting step of the overall adsorption process.
- (3) The negative value of the Gibbs free energy change of the adsorption indicates that the adsorption is spontaneous. The positive value of the enthalpy change of the adsorption shows that the adsorption is an endothermic process. Thus, raising the temperature leads to higher Cu(II) adsorption at equilibrium.

References

1. SHIN S., JANG J. Thiol containing polymer encapsulated magnetic nanoparticles as reusable and efficiently separable adsorbent for heavy metal ions. *Chem. Commun.* pp. 4230-4232, **2007**.
2. BAYTAMOGLU G., ARICA M. Y., BEKTAS S. Removal of Cd(II), Hg(II), and MID ions from aqueous solution using p(HEMA/Chitosan) membranes. *J. Appl. Polym. Sci.* **106**, 169, **2007**.
3. SATHI P., LITINA K., GOURNIS D., GIANOPOULOS T. S., DELIGIANNAKIS Y. *J. Colloid Interface Sci.* **316**, 298, **2007**.
4. BAILEY S. E., OLIN T. J., BRICKA R. M., ADRIAN D. D. A review of potentially low-cost sorbents for heavy metals. *Water Research* **33**, (11), 2469, **1999**.
5. CINCOTTI A., MAMELI A., LOCCI A. M., ORRU R., CAO G. Heavy metals uptake by Sardinian natural zeolites: experiment and modeling. *Industrial & Engineering Chemistry Research* **45**, (3), 1074, **2006**.
6. WU Z. J., JOO H. W., LEE K. T. Kinetics and thermodynamics of the organic dye adsorption on the mesoporous hybrid xerogel. *Chemical Engineering Journal* **112**, 227, **2005**.
7. SOLER-ILLIA G. J., DE A. A., SANCHEZ C., LEBEAU B., PATARIN J. Chemical strategies to design textured materials: from microporous and mesoporous oxides to nanonetworks and hierarchical structures. *Chem Rev.* **102**, 4093, **2002**.
8. LIU Y., PINNAVAIA T. J. Aluminosilicate mesostructures with improved acidity and hydrothermal stability. *J. Mater. Chem.* **12**, 3179, **2002**.
9. STEIN A. Advances in microporous and mesoporous solids highlights of recent progress. *Adv. Mater.* **15**, 763, **2003**.
10. DUBOIS G., REYE C., CORRIU R. J. P., CHUIT C. Organic-inorganic hybrid materials preparation and properties of dibenzo-18-crown-6 ether-bridged polysilsesquioxanes. *J. Mater. Chem.* **10**, (5), 1091, **2000**.
11. IM H. J., YANG Y. H., ALLAIN L. R., BARNES C. E., DAI S., XUE Z. L. Functionalized sol-gels for selective copper (II) separation. *Environ. Sci. Technol.* **34**, (11), 2209, **2000**.
12. KANG T., PARK Y., CHOI K. LEE J. S., YI J. Ordered mesoporous silica (SBA-15) derivatized with imidazole-containing functionalities as a selective adsorbent of precious metal ions. *J. Mater. Chem.* **14**, (6), 1043, **2004**.
13. SAYARIA A., HAMOUDI S., YANG Y. Applications of Pore-Expanded Mesoporous Silica. 1. Removal of Heavy Metal Cations and Organic Pollutants from Wastewater. *Chem. Mater.* **17**, 212, **2005**.
14. ZHAO D., FENG J., HUO Q., NELOSH N., FREDRICKSON G., CHMELKA B., STUCKY G. Triblock Copolymer Syntheses of Mesoporous Silica with Periodic 50 to 300 Angstrom Pores. *Science*, **279**, 548, **1998**.
15. LANGMUIR I. The adsorption of gases on plane surfaces of glass, mica and platinum, *Journal of the American Chemical Society* **40**, 1361, **1918**.
16. FREUNDLICH H. Of the adsorption of gases. Section II. Kinetics and energetics of gas adsorption. Introductory paper to section II, *Transactions of the Faraday Society* **28**, 195, **1932**.
17. SIPS R. On the structure of a catalyst surface, *The Journal of Chemical Physics* **16**, 490, **1948**.
18. ABRAMIAN L., EL-RASSY H. Adsorption kinetics and thermodynamics of azo-dye Orange II onto highly porous titania aerogel. *Chemical Engineering Journal* **2009**.
19. CHIOU M. S., LI H. Y. Adsorption behavior of reactive dye in aqueous solution on chemical cross-linked chitosan beads, *Chemosphere* **50**, 1095, **2003**.
20. CHIOU M. S., LI H. Y. Equilibrium and kinetic modeling of adsorption of reactive dye on cross-linked chitosan beads, *J. Hazard. Mater.* **93**, 233, **2002**.

21. CHANG C. Y., TSAI W. T., ING C. H., CHANG C. F. Adsorption of polyethylene glycol (PEG) from aqueous solution onto hydrophobic zeolite, *J. Colloid Interface Sci.* **260**, 273, **2003**.
22. NOLLET H., ROELS M., LUTGEN P., VAN DER MEEREN P., VERSTRAETE W. Removal of PCBs from wastewater using fly ash, *Chemosphere* **53**, 655, **2003**.
23. SARKAR M., ACHARYA P. K., BHATTACHARYA B. Modeling the adsorption kinetics of some priority organic pollutants in water from diffusion and activation energy parameters, *J. Colloid Interface Sci.* **266**, 28, **2003**.
24. MAK S. Y., CHEN D. H. Fast adsorption of methylene blue on polyacrylic acid-bound iron oxide magnetic nanoparticles, *Dyes Pigments* **61**, 93, **2004**.
25. BHATTACHARYYA K. G., SHARMA A. Azadirachta indica leaf powder as an effective biosorbent for dyes: a case study with aqueous Congo red solutions, *J. Environ. Manage.* **71**, 217, **2004**.
26. YANG X., AL-DURI B. Kinetic modeling of liquid-phase adsorption of reactive dyes on activated carbon, *J. Colloid Interface Sci.* **287**, 25, **2005**.